The Effects of Co^{60} Gamma Radiation on Electron Multiplying Charge-Coupled Devices

Benjamin J. Hadwen, Mercedes Alcon Camas, and Mark S. Robbins, *Senior Member, IEEE*

***Abstract*—Electron multiplying charge coupled devices (EMCCDs) utilize impact ionization to achieve subelectron noise up to video frame rates and above. This paper describes the effects of Co^{60} irradiation on device performance parameters including the dark signal, charge transfer and multiplication gain. Devices were irradiated with different ionizing doses, and biases chosen to simulate operating conditions. The 'global' threshold voltage shift was measured to be around 0.14 V/krad (Si) for all devices. However, the multiplication gain was unchanged by the irradiation. The radiation-induced multiplication register component of dark signal was found to be an order of magnitude larger than that from the image section at room temperature, and to have lower temperature dependence.**

***Index Terms*—Charge-coupled device, Electron multiplying charge coupled device (EMCCD), image sensors, impact ionization, low light, radiation effects.**

I. Introduction

Electron multiplying charge-coupled devices (EMCCDs) utilize impact ionization to achieve high multiplication gain in the charge domain [1]. Consequently performance with an equivalent read-out noise of much less than one electron can be achieved for pixel rates up to and beyond those required for TV imaging applications [2].

The effects of radiation damage on device performance are an important consideration for many potential applications of this new technology. Encouraging results from high-energy proton irradiation of unbiased devices were presented in [3]. In that work, EMCCDs were irradiated unbiased with 6.5 MeV protons to 10 MeV equivalent doses of 5.1×10^8 protons/cm^2 and 2.0×10^9 protons/cm^2. The dark signal generation rate in the read-out and multiplication registers was found to be the same, with no evidence being seen of any field enhancement effects in the multiplication register. However, since the generation of proton-induced dark signal spikes is governed by stochastic processes, it is likely that for a given radiation dose and energy there will be a certain probability of creating a dark signal spike in the multiplication register, caused by an inelastic proton interaction in a high field region of the structure. Further work will be required to determine the statistics of such spike generation.

This present study has been carried out to assess the effects of ionizing radiation on devices running during irradiation. Here, important device performance parameters such as the radiation-induced dark signal, the voltage shift, the multiplication gain, and the ability of the device to transfer charge were assessed following Co^{60} irradiation.

Manuscript received March 6, 2004; revised May 26, 2004.

The authors are with E2V Technologies, Chelmsford, Essex CM1 2QU, U.K. (e-mail: benjamin.hadwen@e2vtechnologies.com; mercedes.alcon.camas@e2vtechnologies.com; mark.robbins@e2vtechnologies.com).

Digital Object Identifier 10.1109/TNS.2004.835099

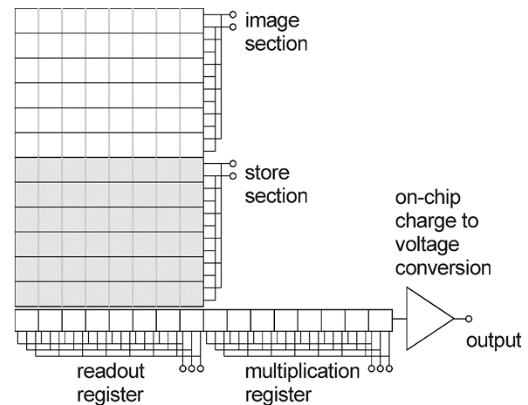

Fig. 1. A schematic layout of the E2V Technologies' EMCCD. It is also possible to include a second conventional output amplifier at the left hand end of the read-out register for added flexibility.

II. Operation and Applications of the EMCCD

Earlier publications have described in detail the construction and operation of the EMCCD (e.g., [2] and [4]).

The sensitivity of a conventional CCD is generally limited by the noise introduced by the on-chip charge to voltage conversion and by processing in the video chain electronics. This read-out noise increases with pixel rate and so applications requiring high sensitivity traditionally utilize a slow read-out rate to minimize the noise. The EMCCD technology effectively eliminates read-out noise by applying gain in the charge domain to increase the signal above the noise floor of the output amplifier. Robbins and Hadwen [4] have shown that the multiplication process increases the input referred noise by a factor of only $\sqrt{2}$ above the ideal input shot noise level.

A schematic layout of an EMCCD is presented in Fig. 1. The image, store, read-out register and output amplifier are of a conventional design, and so would be expected to exhibit radiation damage effects typical of conventional CCDs. The charge multiplication process occurs between the conventional read-out register and the output amplifier in an additional serial register, termed the multiplication register.

Each stage of the multiplication register comprises four gates, three of which are clocked. This is shown schematically in Fig. 2. The gates denoted $\phi 1$ and $\phi 3$ are clocked with normal amplitude drive pulses (amplitude $\sim$10 V) and utilize the same pulses as applied to two phases of the read-out register. Multiplication gain is achieved by the process of impact ionization

0018-9499/04$20.00 © 2004 IEEE

Authorized licensed use limited to: MIT Libraries. Downloaded on July 9, 2009 at 18:37 from IEEE Xplore. Restrictions apply.

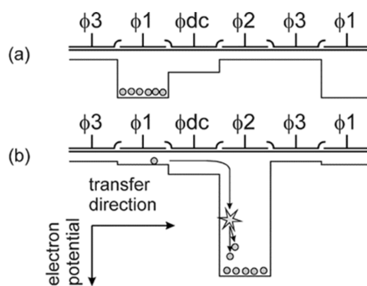

Fig. 2. A schematic of the multiplication element, showing the transfer of charge.

and is controlled by supplying the gate $\phi 2$ with a pulse of approximately 40–45 V amplitude. The gate prior to $\phi 2$, denoted ϕ dc, is held at a low dc level of typically 3 V. By controlling the high level of $\phi 2$, the electric fields can be set sufficiently high so that a proportion of the signal electrons undergo impact ionization as they are transferred from $\phi 1$ to $\phi 2$ during the normal clocking sequence. Thus the number of signal electrons increases as the signal passes through the multiplication element. Although the probability of impact ionization α is low, the number of stages N can be high. Since α is small, the total gain of the cascaded multiplication elements G is given by

$$G = (1+\alpha)^N. \quad (1)$$

For a multiplication register of 600 elements, an α of 0.015 gives a multiplication gain in excess of 7500. The gain is independent of device read-out rate. The typical dependency of gain on $\phi 2$ gate bias and temperature was given in [4].

It can be shown [4] that the total noise referenced to the image area, σ_{eff} is given in the limit of large G by

$$\sigma_{\mathrm{eff}} = \sqrt{2(S + S_{\mathrm{dark}}) + \frac{\sigma^2_{\mathrm{readout}}}{G^2}} \quad (2)$$

where $\sigma_{\mathrm{readout}}$ is the read-out noise, S is the optically generated signal, and S_{dark} is the dark signal. Thus, we see that by setting G to be suitably large we effectively eliminate the effect of the read-out noise on the total noise. By sufficiently cooling the device to eliminate dark signal, the noise can be reduced to within a factor $\sqrt{2}$ of the photon shot noise.

The EMCCD technology has been found to be excellently suited to a diverse range of applications [5]. In real time surveillance imaging applications, the extremely low noise of the sensor facilitates sensitivity performance exceeding that of image intensifiers. The wide interscene dynamic range of the EMCCD enables true 24-h surveillance capability. In the life sciences, EMCCDs have been utilized in the detection of fluorescent and luminescent markers. A ground-based astronomy application has employed an EMCCD to obtain resolutions comparable to those achieved by the Hubble space telescope, and the possibility of operating devices in a photon counting mode has also been demonstrated.

III. Experimental Details

A. Irradiation Details

The device type used for this study was the E2V Technologies' CCD87, a frame transfer EMCCD device with 512×512 square pixels of 16 μm pitch [6]. The gate dielectric is a conventional structure consisting of 85 nm Si_3N_4 on 85 nm SiO_2. Three devices from a single production batch were irradiated. A control device from the same batch was also tested pre- and post-irradiation to account for any radiation independent changes in device or test camera performance.

TABLE I
Radiation Doses Administered

Device number	1st Irradiation Dose (krd (Si))	2nd Irradiation Dose (krd (Si))
1	2	10
2	5	10
3	10	10

The devices were irradiated at the University of Brunel, U.K., during February 2003. The irradiations were conducted in two stages and were tested pre- and post-irradiation, and at the intermediate stage between the first and second irradiations. The time between the first and second doses being administered was 3 wk. Details of the radiation doses supplied are shown in Table I.

Dosimetry was carried out using a calibrated air ionization chamber. The devices under test were positioned approximately 380 mm from the source, so positioning errors were small. The dose rate was approximately 150 rd(Si)/min. The estimated total error in the dosimetry was $\pm 5\%$. The devices were biased during irradiation to best simulate operation, with the substrate bias at $+5$ V, the image and store gate bias at -5 V, the register gate bias at 0 V, and phase $\phi 2$ of the multiplication register clocked with a square wave pulse of low level 0 V and high level 45 V and frequency of approximately 10 kHz (50% duty cycle). Pulsing the $\phi 2$ multiplication register phase ensures that, for the duration of the irradiations, the electric field is switched between the approximate levels corresponding to the clock high and clock low states, for typical operation with $\times 1000$ multiplication gain. The frequency of the applied square wave pulse is not believed to significantly affect the postirradiation performance of the device. The biasing arrangement employed inverts the Si/SiO_2 interface of the image and store sections, but not the read-out or multiplication register structures thus replicating normal operating conditions. The multiplication register is not inverted during normal operation as this would result in hole impact ionization, and thus a high multiplication register dark signal. All amplifier drain connections were biased to their nominal operating values, and the output source was loaded by a suitable resistor to ground. In actual operation the read-out/multiplication register can be clocked up to 15 MHz. However this was not possible during the irradiation due the impedance of the cabling arrangements. The air temperature in the radiation cell was 10 °C. Following irradiation the devices were maintained at room temperature prior to electro optical testing.

B. Device Test Facilities

Two separate test facilities were used to assess device performance before and after radiation. Normally camera 1 was operated at a read-out rate of 11 MHz. Lower read-out rates could be set down to 1 MHz. The device was run in frame transfer mode with a fixed integration time of 30 ms. A resonant sinusoidal clocking scheme was employed to clock phase $\phi 2$ of the multiplication register and facilitate multiplication gain. An electrometer was used to bias the reset drain and measure the cur-

Authorized licensed use limited to: MIT Libraries. Downloaded on July 9, 2009 at 18:37 from IEEE Xplore. Restrictions apply.

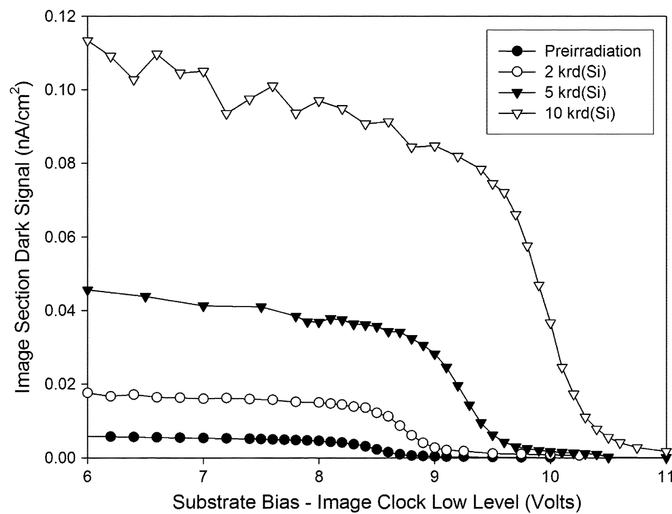

Fig. 3. The measured image section dark signal at -20 °C as a function of substrate bias—image clock low level. Normal operation preirradiation utilizes a substrate bias—image clock low level above 9 V.

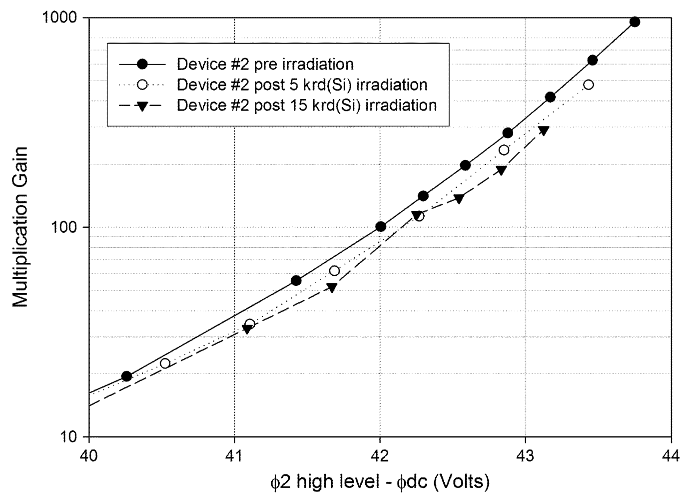

Fig. 4. Measured pre- and postirradiation gain as a function of the $\phi 2$ high level—$\phi\mathrm{dc}$ bias.

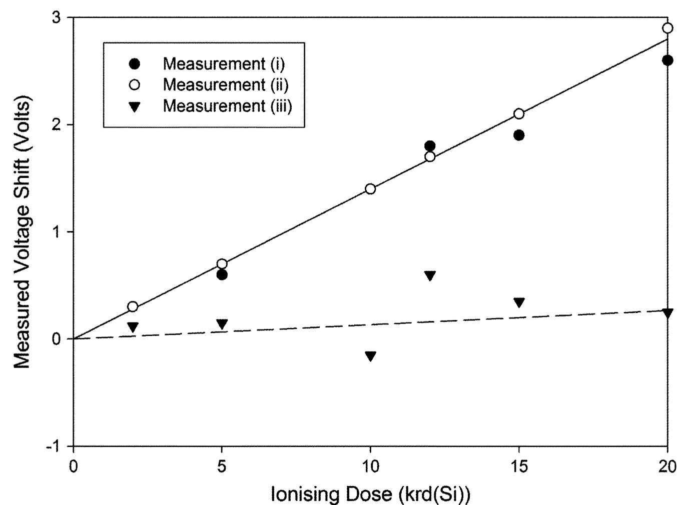

Fig. 5. The voltage shift as a function of ionizing dose, measured using different techniques.

rent down this line. Employing this facility enabled the signal at the output node to be detected to a resolution of 200 electrons/pixel. Calibrated optics were employed to allow attenuation of the light level by various known factors. The device was maintained at the set temperature by means of a Peltier cooled cold finger spring loaded against the back of its ceramic package. The device could be operated at temperatures between $+5$ and $+40$ °C in this camera.

Camera 2 operated at a read-out rate of 1 MHz, with the device being run in frame transfer mode with variable integration times. This camera utilized a square wave clocking scheme to clock phase $\phi 2$ of the multiplication register. The device could be cooled further than in Camera 1 and temperatures down to -55 °C could be set. In both cameras the device temperatures were measured with platinum resistance thermometers in good thermal contact with the ceramic package. The device temperature could be controlled to within ± 1 °C of the required value.

IV. The Effects of Irradiation on Device Performance

A. *Voltage Shift and Multiplication Gain Shift*

It is well known that voltage shifts are induced in devices during irradiation. This is due to the trapping of positive charge in the insulator layers and is a function of the field in the gate dielectrics.

Three different measurement techniques were used to measure the voltage shifts in the different structures of the device.

i) Measurement of the dark signal generated in the image and store sections as a function of the gate to substrate bias using Camera 2. Fig. 3 shows the measured dark signals following different radiation doses. The voltage shift is determined by measuring the change in the gate to substrate bias required to invert the Si at the Si/SiO_2 interface of the image and store sections.

ii) Measurement of the minimum reset drain bias required to successfully attract charge onto the output node (an $\mathrm{n}+$ ohmic contact).

iii) Measurement of the change in the $\phi 2$ high level necessary to maintain the required multiplication gain. To measure the multiplication gain the device was illuminated with a flat field and by measuring the mean signal with and without multiplication gain, the gain could be calculated. This method was described in more detail in [4]. Fig. 4. shows measured multiplication gains as a function of the $\phi 2$ high level, following different radiation doses. A small nonirradiation-induced shift in the $\phi 2$ bias was measured in the control device and has been subtracted from the data in Fig. 4.

The voltage shifts measured using each of these methods are shown in Fig. 5. Measurement using methods i) and ii) give voltage shifts consistent with 0.14 ± 0.01 V/krd(Si) for all devices and method iii) gives a voltage shift of 0.01 ± 0.01 V/krd(Si).

To understand these results the effects of biasing the different structures in the device differently during the irradiation must be considered. As discussed in Section III, the $\phi 2$ phase of the multiplication register was clocked between a small negative gate to

Authorized licensed use limited to: MIT Libraries. Downloaded on July 9, 2009 at 18:37 from IEEE Xplore. Restrictions apply.

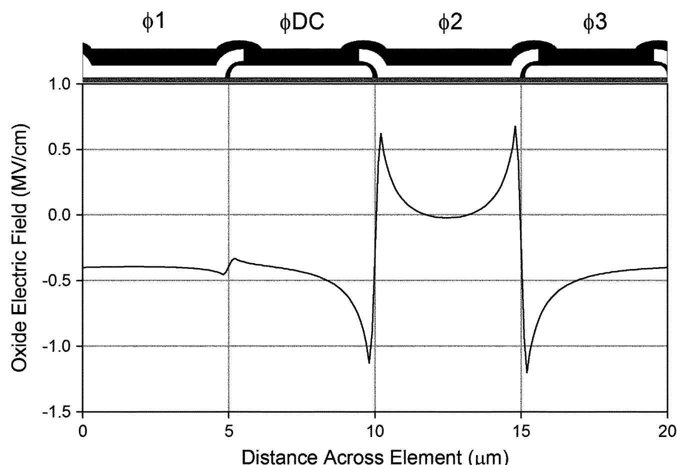

Fig. 6. The calculated electric field in the gate oxide perpendicular to the silicon surface across a 20 μm multiplication element. $\phi2$ is held 45 V.

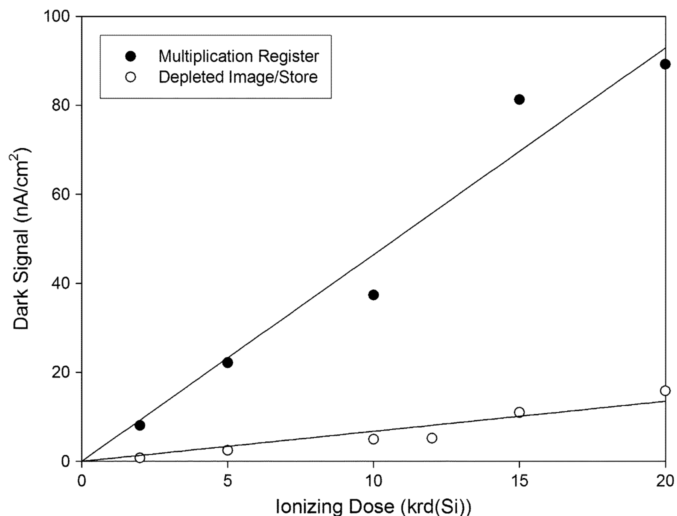

Fig. 7. Readout and multiplication register dark signals as function of dose, measured at 18 °C with a multiplication gain of 100.

substrate bias and a large (40 V) positive bias. The image and store gates, and all the register gates except for $\phi2$ of the multiplication phase, were biased with a negative voltage between gate and substrate.

The high level of the $\phi2$ phase produces significantly different fields in the gate oxide of this phase than in the rest of the device, even when the conventional clocks are at their usual high level. A 2-D simulation of the oxide field in a 20 μm multiplication element, perpendicular to the silicon surface, is shown in Fig. 6. Radiation-induced positive charge created in structures with a negative oxide field will tend to migrate under the influence of the electric field toward the gate and be trapped at the SiO_2/Si_3N_4 interface. This is the situation when conventional clock levels are applied to a buried channel CCD.

Measurements using techniques i) and ii) determine the resultant voltage shift $\Delta V1$. By contrast, positive charge created under the $\phi2$ phase of the multiplication register, when clocked high, will tend to migrate to the SiO_2/Si interface with a resultant voltage shift, $\Delta V2$. The multiplication gain is a function of the difference between the $\phi2$ high level and the adjacent ϕ dc gate bias. Therefore, method iii) is a measurement of the difference in voltage shift between these phases $\Delta V2 - \Delta V1$.

The results of Fig. 5 show that $\Delta V1 \sim \Delta V2$ and thus $\Delta V1 - \Delta V2 \sim 0$ so that the multiplication gain versus $\phi2$ bias characteristic is relatively unchanged by the irradiation. The effect of field strength and direction on voltage shifts using a CCD with a similar Si_3N_4/SiO_2 dielectric was discussed in [7]. Here the voltage shift of a conventional CCD was measured as a function of the potential between the gate and the Si-SiO_2 interface $V_{gate-surface}$. It was shown that the voltage shift was only weakly dependent on this potential when the magnitude of $V_{gate-surface}$ was greater than 5 V, with measurements being made over the range $-18 \leq V_{gate-surface} \leq +10$ V.

To optimally operate a device following irradiation it is necessary to make some adjustment to the operating biases. The substrate bias needs to be increased to successfully suppress the surface dark signal from the image and store sections, as shown in Fig. 3. Irradiated devices also show a shift in the operating point of the output amplifier, leading to a decrease in the output amplifier responsivity. It is possible to recover the responsivity to approximately its preirradiation value by making small increases to the reset drain and output drain biases.

Finally, it should be noted that the CCD87 has a second conventional output amplifier at the opposite end of the read-out register to the multiplication register [6]. It may be necessary to increase the reset drain bias supplied to this amplifier above what was required preirradiation, to avoid the injection of spurious charge from this output amplifier into the read-out register.

B. Radiation-Induced Dark Signal

The image section component of dark signal was measured on camera 1 by setting the multiplication gain to an appropriate value to give a reset drain current of tens of nanoamps. The dark signal was then calculated by measuring this current, and correctly normalizing using the measured multiplication gain. Measurements were also made on camera 2 by obtaining an image after a suitable integration time and subtracting a zero integration time image.

There was no significant increase in the image and store dark signal when running with the surface inverted, i.e., in the normal mode of operation. Depleting the silicon surface reveals the surface component of dark signal that is normally suppressed. The increase in surface dark signal immediately following irradiation is shown in Fig. 3. The radiation-induced component of surface dark signal from the image and store regions was found to be around 10 pA/cm^2/krd(Si) at -20 °C for all devices tested ($\text{substrate bias} - \text{image clock low level} = 8$ V). Similar measurements at a temperature of $+18$ °C showed the radiation-induced component to be 520 pA/cm^2/krd(Si). This measured temperature dependence is in excellent agreement with previous work on E2V (EEV) CCDs [8].

The component of the dark signal arising from the multiplication register were measured on camera 2 by measuring the reset drain current I_{RD} while holding the image and store clocks low to eliminate dark signal components arising from this area. For multiplication gains above about $10\times$, it is straightforward

Authorized licensed use limited to: MIT Libraries. Downloaded on July 9, 2009 at 18:37 from IEEE Xplore. Restrictions apply.

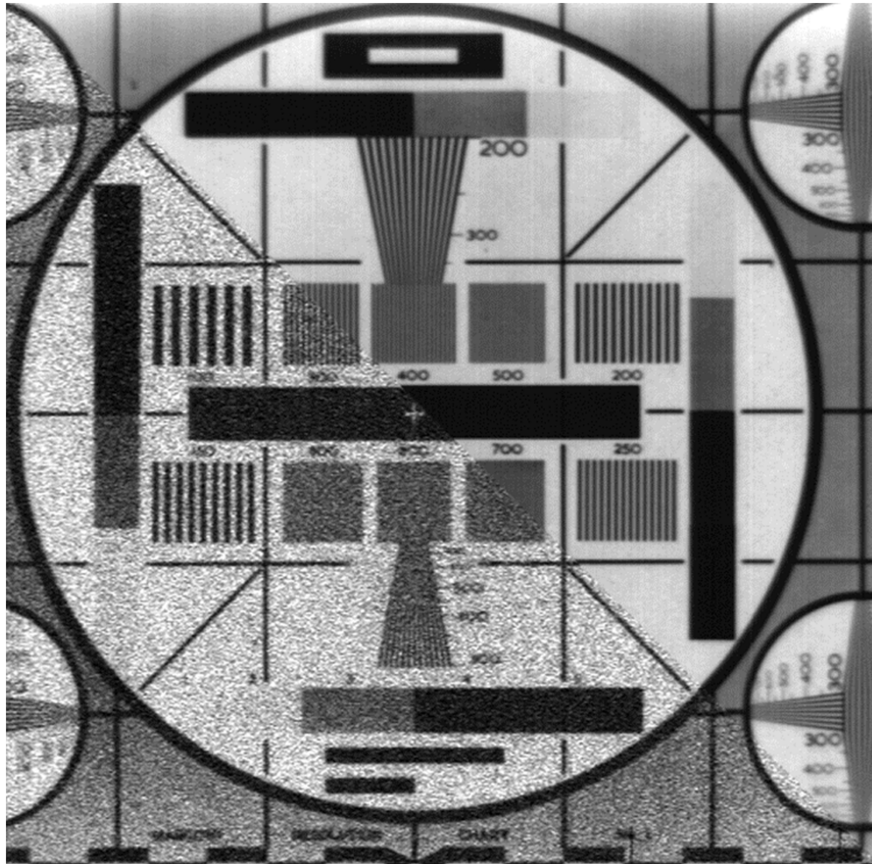

Fig. 8. Two superimposed images of a Test Chart, obtained with an unirradiated device, taken through an $f/1.4$ lens. The mean dark signal is seven electrons per pixel ($T = 10\ ^\circ C$). The top right image is obtained with a mean signal level of 38 ke ($\mathrm{multiplication\ gain} = 1$). In the bottom left image the mean signal level is reduced to 130 electrons ($\mathrm{multiplication\ gain} = 500$). The pixel rate was 11 MHz.

to show that the dark signal generation rate per unit area of the multiplication register, S_M can be calculated from the measured values of I_{RD}, and multiplication gain G using the relationship

$$S_M = \left(\frac{I_{\mathrm{RD}}}{G} - S_R A_R\right) \frac{\ln(G)}{A_M} \tag{3}$$

where A_M and A_R are the areas of a multiplication and read-out register element, respectively, and I_{RD} is a function of G. S_R is the dark signal generation rate per unit area of the read-out register which is assumed to be equal to the image area component. The multiplication register component of dark signal, and thus also the reset drain current I_{RD}, do not scale linearly with the multiplication gain G, as the dark signal generated at different points along the register is amplified by differing numbers of multiplication gain stages. Fig. 7 compares the surface dark signal density from the image and store running out of inversion with that of the dark signal from the multiplication register. In this case, the temperature was $+18\ ^\circ C$ and the gain was set to $100\times$. The read-out rate was 11 MHz. Trials were performed at read-out rates between 3 and 11 MHz and no dependence on frequency was observed. The dark signal generation rate S_M also appears to be independent of multiplication gain. It would in principal be possible to measure the dependence of S_M on the electric field strength by measuring the dark signal for different $\phi 2$ high levels whilst maintaining the $\phi 2 - \phi\mathrm{dc}$ bias constant to keep the multiplication gain constant. However, in practice such a measurement is very difficult since the multiplication gain is a very rapid function of the $\phi 2 - \phi\mathrm{dc}$ bias, while the electric field varies much more weakly over the range of adjustment for which this is possible.

The fact that the radiation-induced dark signal density from the multiplication register is significantly higher than the surface component from the conventional parts of the device may be due to the direction of hole motion in the gate oxide during irradiation. Alternatively, it may be due to field enhanced emission effects. This latter hypothesis appears to be backed up by the lower temperature dependence than is usually observed for radiation-induced surface dark signal.

C. Charge Transfer

A detailed study of the charge transfer efficiency (CTE) was beyond the scope of the current paper. However, to facilitate a qualitative evaluation chart images were obtained over a range of illumination levels. Two images are presented in Fig. 8 from an unirradiated device, and for comparison, two images from an irradiated device are given in Fig. 9, under the same conditions. The devices were operated using camera 1 at $10\ ^\circ C$, running at a pixel rate of 11 MHz and a frame time of 30 ms.

Due to the direction of the field experienced by signal electrons, it may be expected that some of these signal electrons will come into contact with the SiO_2/Si interface under the $\phi 2$ phase

Authorized licensed use limited to: MIT Libraries. Downloaded on July 9, 2009 at 18:37 from IEEE Xplore. Restrictions apply.

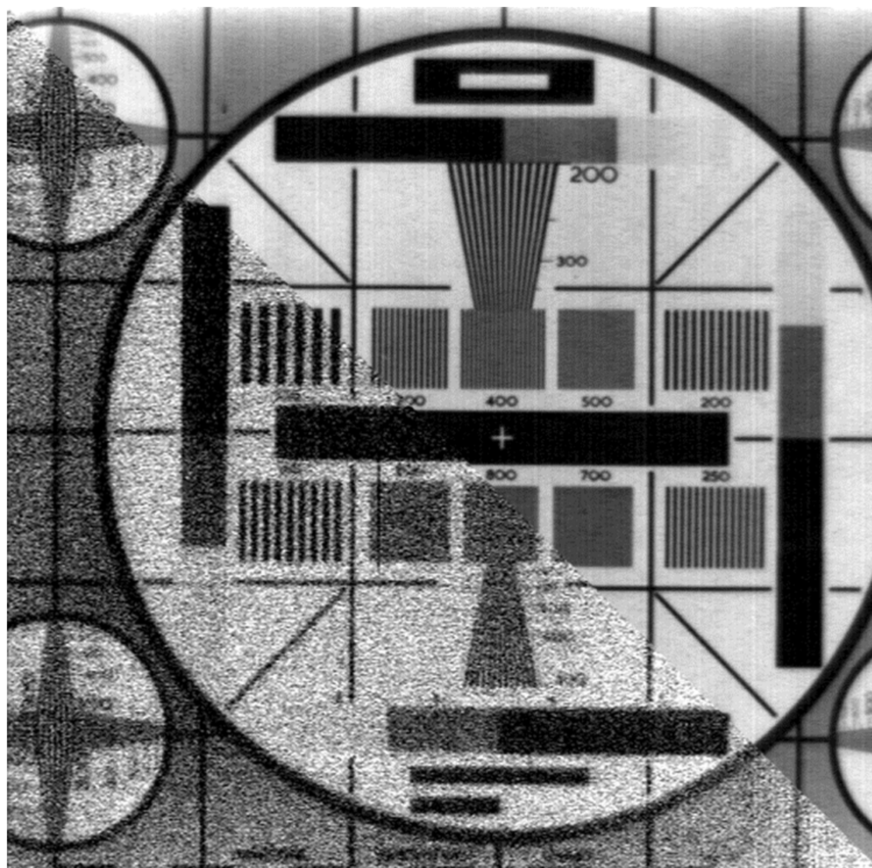

Fig. 9. Two images obtained after 12 krd(Si), under the same conditions as Fig. 8. The mean dark signal is 170 electrons per pixel ($\mathrm{T} = 10\ ^\circ\mathrm{C}$). The top right image is obtained with a mean signal level of 38 ke ($\mathrm{multiplication\ gain} = 1$). In the bottom left image the mean signal level is reduced to 130 electrons ($\mathrm{multiplication\ gain} = 500$).

of the multiplication register. Therefore, it would be reasonable to expect the CTE to be a function of the density of radiation-induced states created at this interface. However, qualitative assessment of the CTE viewing the test chart images shows no obvious degradation as a result of the irradiation: respectable imaging performance is obtained, even after quite large ionizing doses have been administered. There is no evidence that any potential pockets were generated and the increase in interface state density in the multiplication register did not appear to significantly affect the CTE.

V. Discussion

The results of this study, together with the work presented in [3], shows that the performance of the EMCCD following irradiation is sufficiently promising to merit the consideration of this technology for use within radiation environments. The suitability of the technology will depend largely on the ability to reduce the dark signal by cooling and by the signal levels to be detected. Further work is required to fully understand the degradation mechanisms, especially the dark signal generated within the multiplication register.

Acknowledgment

The authors thank Prof. A. Holmes-Siedle and the University of Brunel for their assistance in carrying out the irradiations.

References

[1] S. K. Madan, B. Bhaumik, and J. M. Vasi, “Experimental observation of avalanche multiplication in charge coupled devices,” *IEEE Trans. Electron Devices*, vol. ED-20, pp. 694–699, 1983.

[2] P. Jerram *et al.*, “The LLCCD: Low light imaging without the need for an intensifier,” in *Proc. SPIE*, vol. 4306, 2001, pp. 178–186.

[3] D. R. Smith, A. D. Holland, and M. S. Robbins, “The effect of protons on E2V technologies’ L3Vision CCDs,” *Nucl. Instrum. Methods*, vol. A513, pp. 296–299, 2003.

[4] M. S. Robbins and B. J. Hadwen, “The noise performance of electron multiplying charge coupled devices,” *IEEE Trans. Electron Devices*, vol. 50, pp. 1227–1232, May 2003.

[5] CCD87 Front Illuminated Device Datasheet [Online]. Available: http://e2vtechnologies.com/introduction/prod_l3vision.htm

[6] e2v technologies—L3Vision—Introduction [Online]. Available: http://e2vtechnologies.com/datasheets/l3vision_ccds/ccd87-00_fi_4p_imo.pdf

[7] M. S. Robbins *et al.*, “Quality control and monitoring of radiation damage in charge coupled devices at the stanford linear collider,” *IEEE Trans. Nucl. Sci.*, vol. 40, pp. 1561–1566, 1993.

[8] T. Roy, “Ionising radiation induced surface effects in charge coupled devices,” Ph.D. dissertation, Brunel University, Uxbridge, Middlesex, U.K., Sept. 1993.

Authorized licensed use limited to: MIT Libraries. Downloaded on July 9, 2009 at 18:37 from IEEE Xplore. Restrictions apply.